

Brain Tumor Classification and Segmentation Using Deep Convolutional Neural Networks

Deep Learning - Final Project Report

Abner Farrel J. Hamonangan

Simanjuntak

(21/477685/PA/20686)

Department of Computer Science and Electronics, Universitas Gadjah Mada

Building C, 4th Floor North

Yogyakarta, Indonesia

abner.far2003@mail.ugm.ac.id

Peter Johan Arkadhira Setiabudi

(21/475025/PA/20510)

Department of Computer Science and Electronics, Universitas Gadjah Mada

Building C, 4th Floor North

Yogyakarta, Indonesia

peter.johan0403@mail.ugm.ac.id

Rabbani Nur Kumoro

(21/472599/PA/20310)

Department of Computer Science and Electronics, Universitas Gadjah Mada

Building C, 4th Floor North

Yogyakarta, Indonesia

rabbani.nur.kumoro@mail.ugm.ac.id

Abstract — Brain tumors pose a significant threat to human health, demanding precise detection and handling. Currently used approaches suffer from dependence on human interpretation, which is prone to human error, and require skilled radiologists which are few in number. To address these challenges, this study proposes a solution that uses Convolutional Neural Network (CNN) architectures for precise tumor classification and segmentation. The proposed methodology employs EfficientNet for the classification phase and U-Net for the segmentation phase. The approach achieves impressive results, with accuracy reaching 99% and an IoU score of 89%, showcasing its effectiveness in accurately classifying and segmenting tumor regions. By leveraging advanced CNN architectures and semantic segmentation techniques, this solution aims to overcome limitations, provide a more reliable method for brain tumor diagnosis, and enable early detection of brain tumors, thus supporting effective medical strategies.

Keywords — *Brain Tumor Diagnosis, Cancer, Deep Learning, Medical Imaging, MRI*

I. INTRODUCTION

A brain tumor is an abnormal growth of cells within the brain or central nervous system, with potential classifications as benign or malignant. These growths can occur in various brain or spinal cord regions and are influenced by factors such as genetic mutations, radiation exposure, and immune system disorders. Despite their relatively low global prevalence, less than 2% of all cancers, brain tumors present a significant health challenge, having the lowest survival rate among all cancer types, as reported by the World Health Organization (WHO) [1]. Regional variations in tumor types are observed, with benign meningiomas being predominant in 40-60% of cases in Indonesia, while malignant Gliomas are more prevalent in Europe and America [2].

Brain tumors manifest in diverse forms, commonly categorized as either cancerous or non-cancerous. A benign tumor, characterized by slow growth and confinement to the brain, does not affect other cells in the body and can be identified and treated in its early stages. Conversely, malignant tumors, classified into primary and secondary types, are cancerous [3]. A primary malignant tumor originates in the brain, while a secondary or metastatic tumor initially appears elsewhere in the body and then spreads to the brain. Among the frequently diagnosed brain tumors are meningioma, glioma, and pituitary cancer.

Meningioma takes its name from the three membranes surrounding the brain and spinal cord, where it develops. Glioma tumors arise from glial cells, which support the functioning of nerve cells. In cases where glioma exhibits aggressive growth and infiltrates normal nerve cells, the inpatient survival rate is limited to a maximum of two years. The pituitary, a small gland located at the back of the nose, undergoes abnormal proliferation, impacting various brain glands and numerous bodily processes [4].

Accurate analysis of the unique characteristics of brain tumors during the initial stages is imperative. This precision enables physicians to make informed decisions regarding the most suitable treatment options, critically influencing the patient's chances of survival. However, the challenge lies in recognizing and classifying these tumors early on, given the complexities introduced by factors such as asymmetrical shapes, diverse textures, varied locations, and indistinct borders. The proposed study involves employing a classification and segmentation approach, utilizing the EfficientNet and U-Net Convolutional Neural Network (CNN) architecture for tumor classification and segmentation. The objective of this study is to formulate refined classification and segmentation methods that effectively identify tumors and facilitate the early detection of brain tumors.

II. PROBLEM STATEMENTS

The imperative to detect brain tumors early is underscored by the existing diagnostic methods relying on subjective judgments, resulting in inconsistent diagnoses. The complexity of diagnosing brain tumors, often asymptomatic, poses challenges for even advanced tools like magnetic resonance imaging (MRI) scans to distinguish them from healthy tissue. Automatic segmentation and classification of medical images play an important role in diagnostics, growth prediction, and treatment of brain tumors.

An early tumor brain diagnosis implies a faster response in treatment, which helps to improve the patient's survival rate. Location and classification of brain tumors in large medical image databases, taken in routine clinical tasks by manual procedures, have a high cost both in effort and time. An automatic detection procedure is desirable and worthwhile. The intricacies extend to identifying the specific tumor type, emphasizing the need for an automated model to enhance the speed and precision of tumor identification. In response to this challenge, deep learning

methods are employed, playing a pivotal role in automating the classification, and segmentation processes. The integration of deep learning facilitates efficient and accurate analysis of medical images, significantly reducing the time and effort traditionally associated with manual procedures.

III. LITERATURE STUDY

The literature review in the proposed study is focused on leveraging deep learning, particularly CNNs, for brain tumor classification and segmentation. The primary objective is to examine the effectiveness of CNNs in these tasks, drawing insights from recent real-life studies.

One noteworthy study, conducted by [5], utilized Dense Efficient-Net for brain tumor classification, achieving an impressive 98.78% accuracy across four tumor categories. Another significant contribution by [6] employed the VGG16 network on the BRATS Kaggle dataset, attaining a commendable 96.70% accuracy in distinguishing malignant and benign tumors. Additionally, [7] focused on multi-class tumor identification, training a CNN on 3064 T1-weighted contrast-enhanced MRI images. Their approach yielded a notable 94% accuracy.

In the segmentation studies conducted by [8], the BraTS 2018 dataset served as the foundation, involving a preprocessing step that removed 1% of the highest and lowest intensities, followed by the normalization of each modality of MR images. To address class imbalance, various data augmentation techniques were applied. The segmentation models employed in these studies were grounded in CNN architectures, designed similarly to U-net. The evaluation of segmentation accuracy was conducted using the dice coefficient, resulting in scores of 0.717, 0.867, and 0.798 for enhanced tumor, whole tumor, and core tumor detection, respectively.

In a different approach by [9], the focus was on automatic brain tumor detection and segmentation using the U-Net architecture applied to the BraTS 2015 dataset. The normalization process encompassed subtracting the mean and dividing by the standard deviation for each sequence of multimodal MRI images. The evaluation strategy incorporated a five-fold cross-validation method for both HGG and LGG data. The segmentation performance demonstrated noteworthy dice coefficients of 0.86, 0.86, and 0.85 for the complete tumor region, core tumor region, and enhancing tumor region, respectively.

Nevertheless, it is crucial to acknowledge and delve into specific limitations inherent in the studies discussed. Firstly, the segmentation methods were rigorously evaluated using a cross-validation scheme, which undoubtedly ensures an unbiased predictor. However, to attain a more comprehensive and objective assessment, additional validation on a distinct and independent testing dataset could be considered. This approach would provide a more robust evaluation of the segmentation models' performance in real-world scenarios. Secondly, the studies underscore the significance of meticulous parameter tuning within the network to augment the robustness and generalizability of the segmentation model. This emphasizes the need for a nuanced understanding of the interplay between various parameters to fine-tune the model for optimal performance. These considerations, though presenting challenges, also highlight areas for potential refinement and optimization in future research endeavors. Despite these acknowledged

limitations, the collective insights from these studies emphasize the adaptability and efficacy of CNN architectures, offering valuable perspectives that contribute significantly to the ongoing exploration of brain tumor classification and segmentation in the proposed study.

IV. METHODOLOGY

The methodology employed in this study involves a comprehensive process for the classification and segmentation of various brain tumors from a diverse set of MRI images. The procedure begins with loading and preprocessing an MRI scan. Subsequently, the CNN architecture, specifically EfficientNet, is utilized to classify the images into four distinct classes: Meningioma, Glioma, Pituitary, and No Tumor. Following the classification phase, the segmentation task is executed using U-Net. This segmentation process aims to delineate and highlight the specific regions within the classified images where tumors are present, providing a detailed understanding of the tumor boundaries and aiding in precise localization. This comprehensive overview, as depicted in **Figure 1**, delineates the systematic approach employed for the classification and segmentation of tumor regions in MRI images.

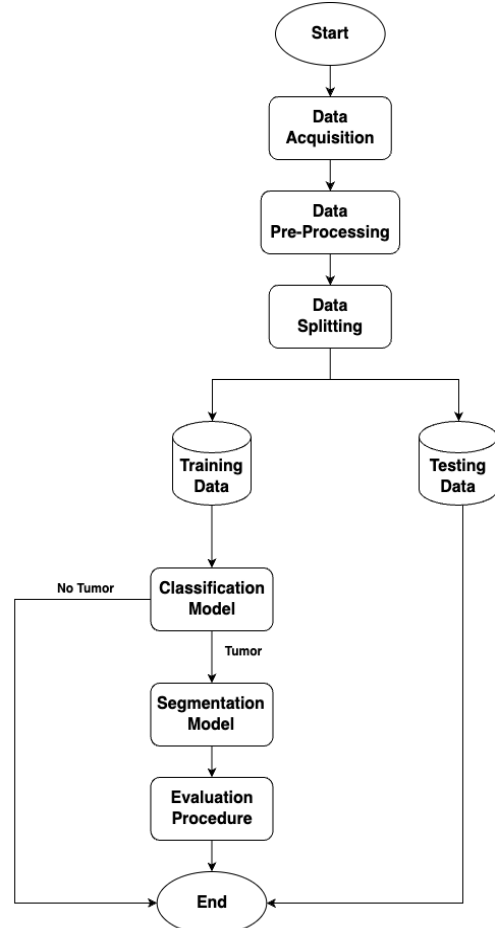


Figure 1. Methodology Flowchart Diagram

A. Classification Data Acquisition

The dataset employed for our classification model is the "Brain Tumor MRI Dataset," obtained from Kaggle. This dataset underwent careful curation with the explicit goal of creating a robust model capable of recognizing brain tumor images, with a primary emphasis on achieving multi-class classification [10].

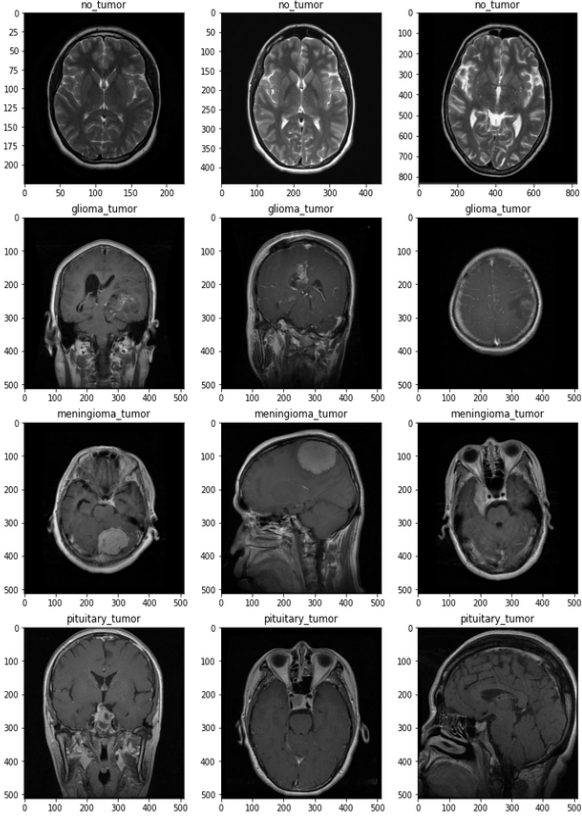


Figure 2. Samples from Brain Tumor MRI Dataset

The dataset showcased in **Figure 2** encompasses four distinct classes: glioma, meningioma, no tumor, and pituitary, constituting a total of 7023 human brain MRI images. To enhance diversity and comprehensiveness, the dataset consolidates information from three primary sources: Figshare, SARTAJ Kaggle, and Br35H Kaggle datasets. It's worth noting that images representing the "no tumor" class were exclusively sourced from the Br35H dataset. Nevertheless, challenges arose from the SARTAJ dataset, particularly concerning the misclassification of glioma class images. This issue was identified through cross-referencing with other research outcomes and diverse model training. Consequently, the problematic images were systematically excluded, and alternative images from the Figshare site were incorporated. This meticulous curation is undertaken with the primary objective of establishing a reliable foundation for the training of the classification model, ensuring precise identification and differentiation of various brain tumor types.

B. Segmentation Data Acquisition

The dataset utilized for segmentation in this study is the Kaggle Brain Tumor Segmentation Dataset, which includes high-resolution 2D MRI images depicting brain tumors [11]. Each image is accompanied by a corresponding mask or ground truth prediction, outlining the boundaries of the tumor. The dataset is extensive, comprising a total of 3064 MRI slices. It encompasses diverse tumor types, such as meningiomas, gliomas, and pituitary tumors. These images are captured from common perspectives, including sagittal, coronal, and axial views. Visual examples of the datasets are presented in **Figure 3**.

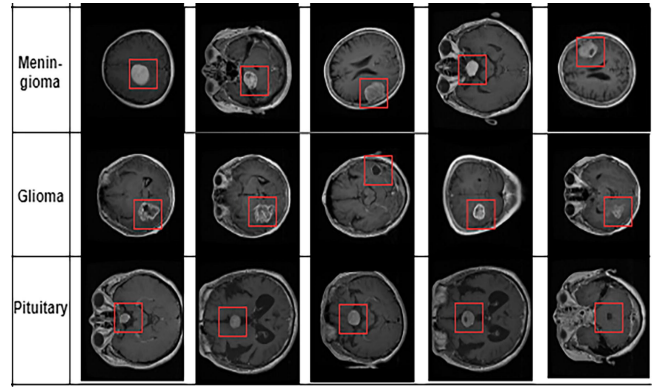


Figure 3. Samples from Brain Tumor Segmentation Dataset

C. Image Data Pre-Processing

Upon acquiring the data, a series of preprocessing steps are employed to optimize the dataset for subsequent analysis. The first step involves grayscaling, which converts the images to grayscale. This conversion of the MRI images to grayscale serves to accentuate the intensity information present in the scans. By focusing on intensity variations rather than color, the subsequent analysis becomes more robust in detecting subtle differences indicative of underlying conditions.

Following this, bilateral filtering is applied to preserve intricate structures while mitigating noise in the images. In the context of brain tumor analysis, where precise structural information is crucial for accurate classification and segmentation, bilateral filtering helps maintain the integrity of intricate features within the scans.

Pseudocoloring techniques are then utilized to enhance the visualization of specific image characteristics. This step aims to highlight particular details or abnormalities that may be critical for accurate tumor identification and segmentation. Pseudocoloring aids in creating a more visually interpretable representation of the data, potentially revealing patterns that might be challenging to discern in grayscale.

Subsequently, all images are resized to a standardized resolution of 256x256 pixels. This step is pivotal for ensuring consistency in image dimensions across the dataset. Standardization simplifies the subsequent analysis and allows for the seamless integration of the images into the model, promoting a uniform understanding of features and patterns associated with different tumor types.

Normalization is applied to scale pixel values to a common range. This step is essential for facilitating the learning process of the model. By standardizing pixel values, the model becomes more adept at recognizing patterns and variations across the dataset, contributing to a faster and more accurate classification and segmentation of brain tumors. The results of the preprocessing results are presented in **Figure 4**.

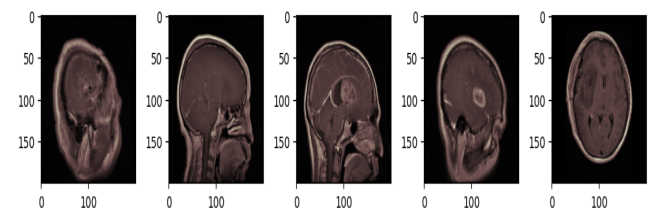


Figure 4. Data Preprocessing Results

Lastly, data augmentation techniques are implemented to diversify the dataset by creating variations of existing images, such as rotations or flips. This augmentation enhances the model's ability to learn from different perspectives and positions, ultimately contributing to its overall versatility in handling varied input scenarios. The variations of the data augmentation techniques are presented in **Figure 5**.

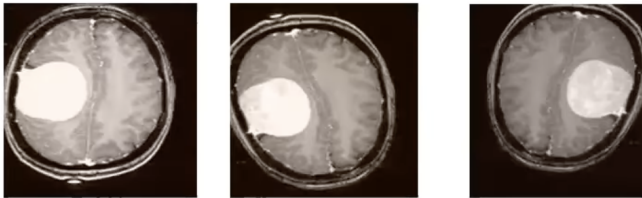


Figure 5. Examples of Data Augmentation Process

D. Classification Modeling

In our approach, we implement classification as a means to enhance the accuracy of brain tumor segmentation. Performing classification will help to differentiate different types of brain tumors which in turn will assist in the segmentation process. To develop the classification model, we will utilize the EfficientNet architecture. It is a type of CNN architecture and scaling approach that uniformly adjusts the dimensions of depth, width, and resolution by applying a compound coefficient as shown in **Figure 6**. In contrast to traditional methods that independently scale these factors, EfficientNet's scaling method maintains a consistent and proportional adjustment of network width, depth, and resolution through a predefined set of scaling coefficients [12].

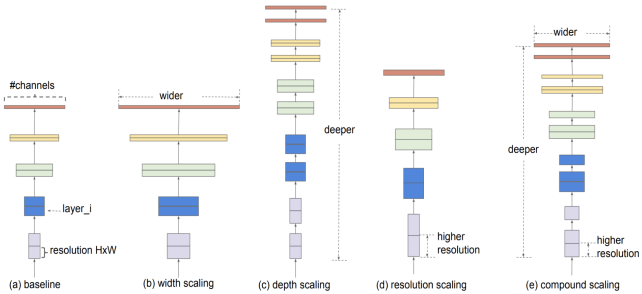


Figure 6. EfficientNet Model Scaling

EfficientNet is well-suited for medical image classification due to its efficiency in extracting and learning distinctive features from medical images, its smaller size with fewer parameters, and its ability to generalize well on transfer learning datasets. Research has shown that fine-tuning EfficientNets on medical imaging classification tasks can lead to high accuracy [13].

We will perform classification using two different variations of EfficientNet. Namely EfficientNetB0 and EfficientNetB3. The main differences between the variants are the computation time and the size of input images. We chose these two variations specifically because they are the low and mid-range options for the EfficientNet architecture.

1. EfficientNetB0

EfficientNetB0 is the base model of the EfficientNet family, and it is trained on more than a million images from the ImageNet database [14]. The model can be used for image classification

tasks and is often used as a starting point for transfer learning. The model architecture for EfficientNetB0 can be seen in **Figure 7**.

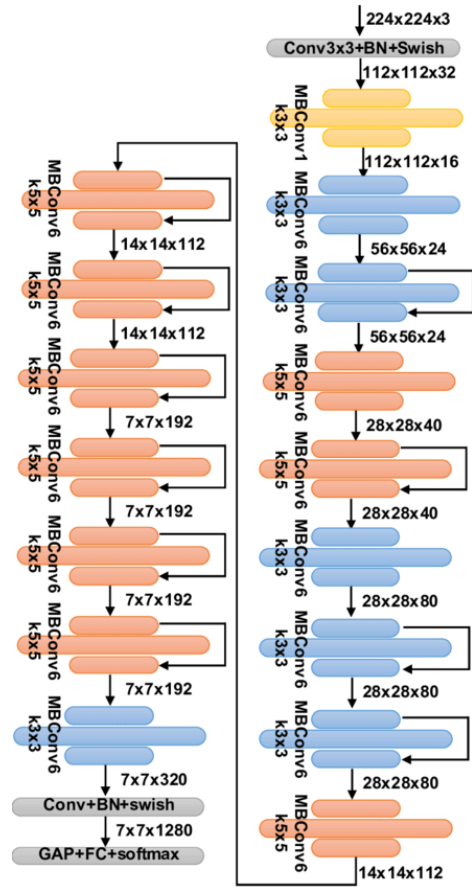


Figure 7. EfficientNetB0 Architecture

2. EfficientNetB3

EfficientNetB3 is a smaller and faster version of the EfficientNet architecture, which can be used for smaller models and faster training. These models are designed to be more efficient in terms of parameters and computational resources while maintaining high accuracy [15]. The model architecture for EfficientNetB3 can be seen in **Figure 8**.

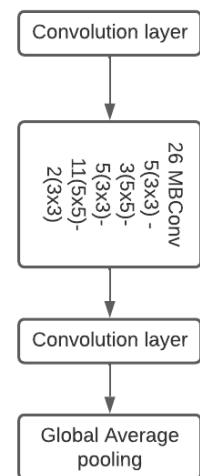


Figure 8. EfficientNetB3 Architecture

E. Segmentation Modeling

In this study, we employ the state-of-the-art U-Net model, specifically designed for biomedical image segmentation [16], to accomplish this task effectively, the model architecture is shown in **Figure 9**. The model was trained by employing an 80/20 train-validation split and throughout 20 epochs. To prevent overfitting and ensure generalization, an early stopping mechanism was employed.

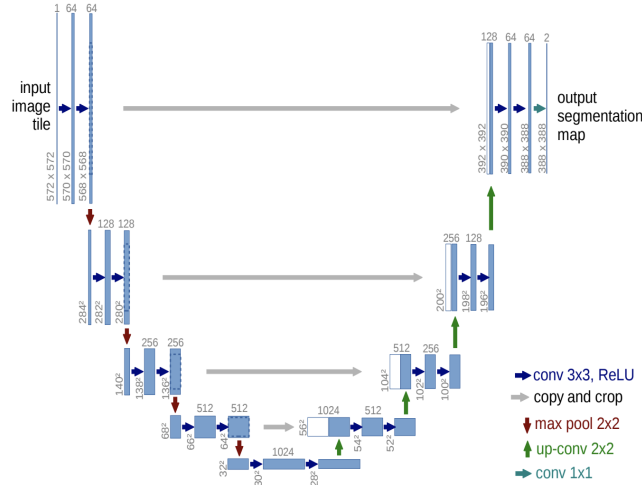


Figure 9. U-Net Architecture

The network consists of a contracting path, known as the encoder, a bottleneck, and an expansive path, known as a decoder, which gives it the “U” shaped architecture. The contracting path functions as a typical convolutional network, involving repeated convolution operations followed by rectified linear units (ReLU) and max-pooling operations. This process, known as contraction, reduces spatial information while enhancing feature information. The bottleneck connects the encoder and decoder, serving as a bridge for combining both types of information. The expansive path involves a series of up-convolutions and concatenations with high-resolution features from the contracting path. This mechanism facilitates the integration of high-level semantic information from the encoder with detailed spatial information from the decoder, ensuring a comprehensive understanding of the input data [17].

This unique architecture allows the U-Net to effectively segment tumor regions in medical images. The contracting path's convolutional operations enable the encoder to capture intricate features related to tumor characteristics, providing a high-level understanding of the input image. The bottleneck ensures the seamless transfer of both feature and spatial information to the decoder. The expansive path, through up-convolutions and concatenations, reconstructs the spatial details while incorporating high-resolution features.

F. Results

The performance of the EfficientNet models in tumor classification is evident from the obtained results, as illustrated in the confusion matrices depicted in **Figure 10** and **Figure 11**. These matrices reveal minimal misclassifications, underscoring the models' effectiveness in identifying and categorizing tumor classes. In the EfficientNetB0 models, only three glioma, two meningioma, one non-tumor, and two pituitary classes were misclassified.

In the EfficientNetB3 model, only four gliomas, two meningiomas, one non-tumor, and two pituitary classes were misclassified. This exemplary performance demonstrates the models' remarkable capability to accurately discern each tumor class, emphasizing their precision, reliability, and suitability for robust tumor classification tasks.

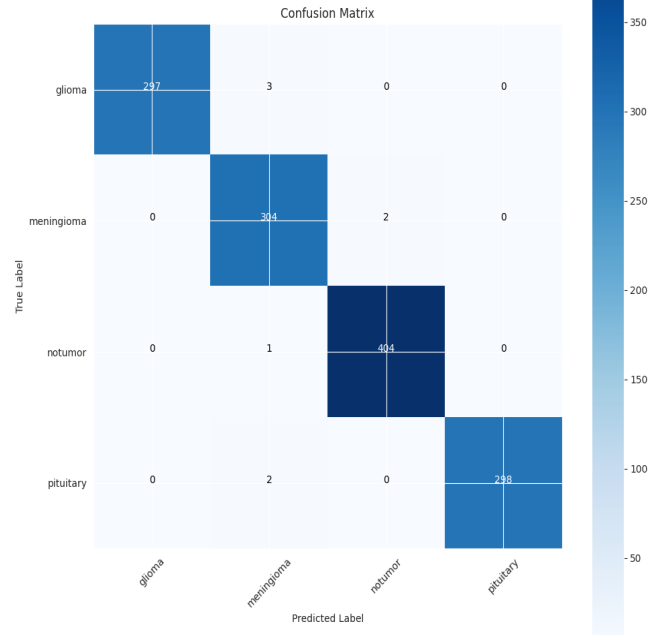


Figure 10. Confusion Matrix of EfficientNetB0

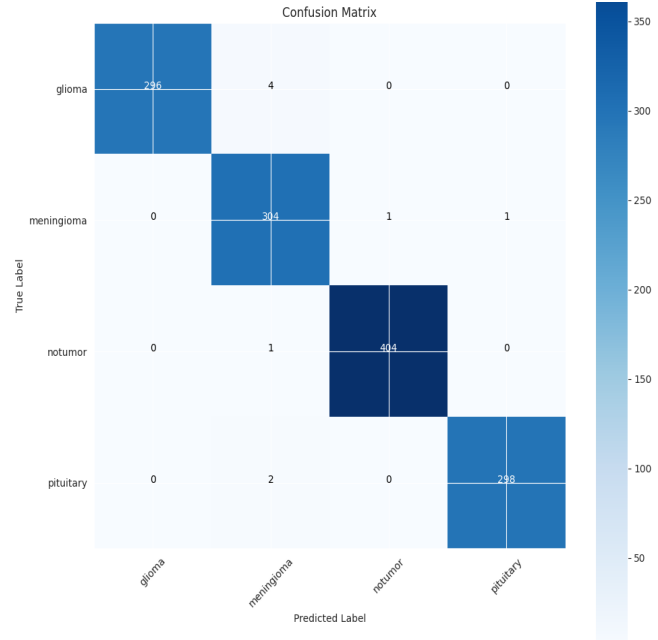


Figure 11. Confusion Matrix of EfficientNetB3

The segmentation results derived from the U-Net model affirm its efficacy in the accurate identification and delineation of tumor regions, as vividly illustrated in **Figure 12**. These visualizations showcase the model's ability to minimize false positive segmentations, ensuring a close alignment of the identified tumor areas with the ground truth labels. This level of precision is indicative of the model's robust capability to capture intricate details in tumor

boundaries, demonstrating its accuracy and reliability in the demanding task of tumor segmentation.

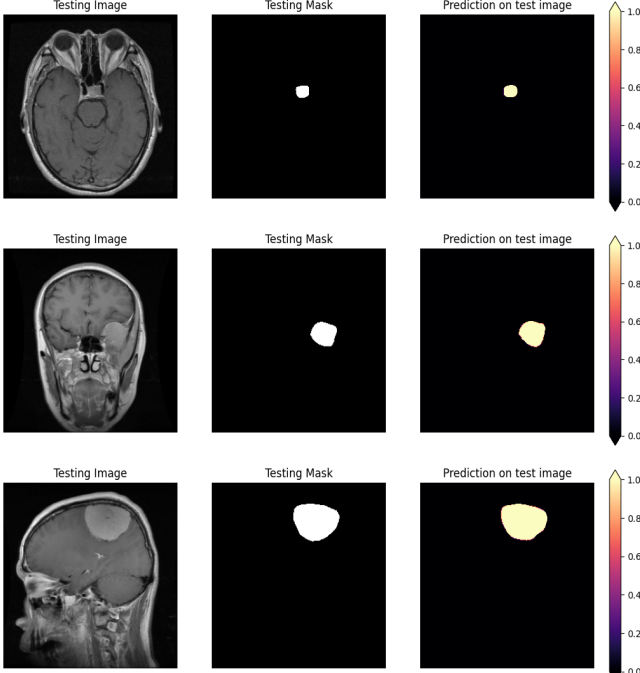


Figure 12. Segmented Tumor Region Results

V. PERFORMANCE EVALUATION

The metrics utilized in the classification report outlined in **Table 1**, which encompass accuracy, recall, precision, and F1-score, are widely employed for assessing the performance of classification models. Accuracy gauges the overall correctness of the model's predictions, while recall measures the model's capacity to correctly identify all instances of the positive class. Precision evaluates the ratio of accurately predicted positive instances to all predicted positive instances. The F1-score offers a balanced assessment, taking into account both precision and recall, making it a suitable metric for comprehensive classification model evaluation.

Table 1. Classification Report

Model	Accuracy	Recall	Precision	F1-Score
EfficientNetB0	99.39%	0.99	0.99	0.99
EfficientNetB3	99.31%	0.99	0.99	0.99

EfficientNetB0 demonstrates an outstanding accuracy of 99.39%, signifying a remarkable correctness in its portrayal of brain tumors. With a recall of 0.99, the model exhibits a robust ability to identify nearly all instances of the positive class, underlining its effectiveness in capturing relevant positive instances. The precision of 0.99 indicates that the majority of instances predicted as positive by the model are indeed true positives. The F1-score, standing at 0.99, further emphasizes the model's excellent balance between precision and recall, reflecting its overall robust performance in brain tumor classification. Notably, EfficientNetB3 yields comparable results to EfficientNetB0, boasting an accuracy of 99.31%, along with identical recall, precision, and F1-Score values of 0.99.

While the models share similar performance metrics, the primary distinction lies in accuracy, where EfficientNetB0

slightly outperforms EfficientNetB3 by 0.08%. This discrepancy is attributed to the larger and more complex architecture of EfficientNetB3 compared to EfficientNetB0, coupled with the implementation of an equal number of epochs for both models.

As shown from the learning curves presented in **Figure 13** and **Figure 14**, it can be seen that both the EfficientNetB0 and EfficientNetB3 models' learning curves are quite similar. The loss for both models is identical, while the model accuracy shows a minor difference in the curves with the EfficientNetB3 model having a bigger gap between the training and testing curves.

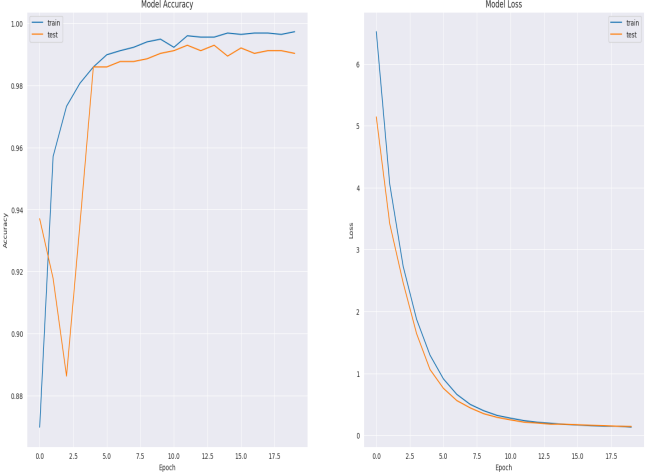


Figure 13. EfficientNetB0 Learning Curves

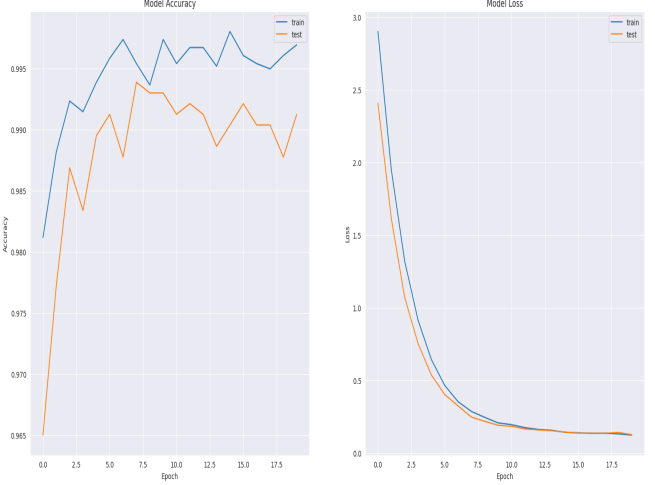


Figure 14. EfficientNetB3 Learning Curves

In the segmentation report detailed in **Table 2**, the metrics employed, namely accuracy, IoU score, dice loss, and focal loss, are tailored to the specific demands of semantic segmentation tasks. Accuracy assesses the accuracy of the model's pixel-wise predictions. Intersection over Union (IoU), quantifies the overlap between the predicted segmentation masks and the corresponding ground truth masks, providing a metric for segmentation accuracy. The dice coefficient measures the resemblance between predicted and ground truth masks.

Table 2. Segmentation Report

Model	Accuracy	IoU	Dice Coefficient
U-Net	99.97%	0.890	0.905

The U-Net model exhibits an impressive accuracy of 99.97%, underscoring its exceptional proficiency in delivering correct segmentation predictions. This high accuracy reflects the model's robust ability to precisely identify and delineate tumor regions within the MRI images. Furthermore, the IoU score, standing at 0.89, signifies a remarkable degree of overlap between the predicted and ground truth masks. This metric, known for quantifying the spatial agreement between the segmentation output and the actual tumor boundaries, highlights the model's capacity to accurately capture and align with the intricate contours of tumor regions.

In addition to its high accuracy and IoU score, the U-Net model achieves a noteworthy Dice Coefficient score of 0.905. The Dice Coefficient, measuring the similarity between the predicted and ground truth masks, attests to the model's precision in delineating tumor boundaries. The elevated Dice Coefficient score further accentuates the model's excellence in capturing fine details and nuances in tumor segmentation, consolidating its reputation for accuracy and reliability in this critical task.

The learning curve depicted in **Figures 15, 16, and 17** for the U-Net models provides valuable insights into the model's training dynamics. Notably, the curves exhibit a characteristic behavior indicative of a well-generalized model, as there is no evident overfitting. The consistent performance across epochs, as illustrated in the learning curves, further reinforces the reliability and stability of the U-Net models in capturing complex relationships within the data without succumbing to the pitfalls of overfitting.

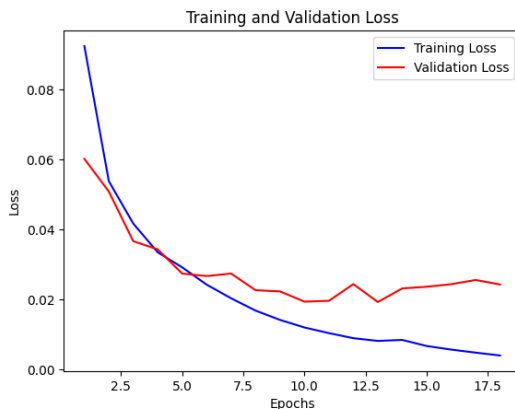


Figure 15. Train and Validation Loss Result

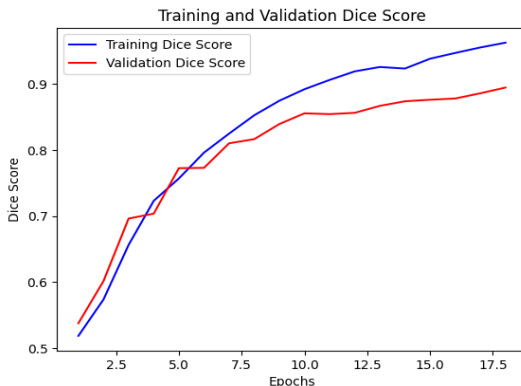


Figure 16. Train and Validation Dice Result

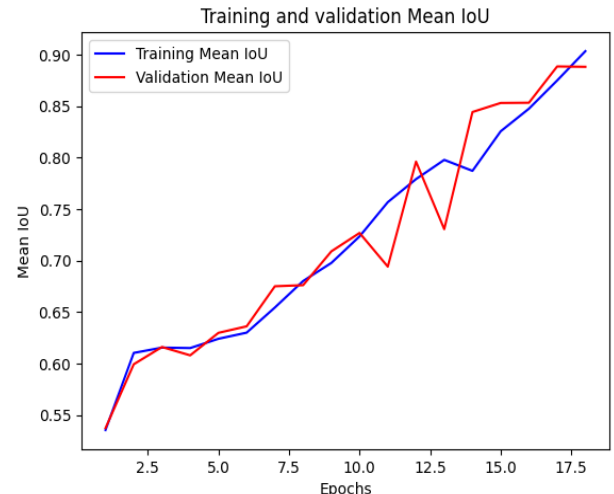


Figure 17. Train and Validation IoU Result

Despite the results, there is room for improvement in the IoU score. To surpass the 0.90 threshold, it is crucial to implement strategic adjustments in the U-Net model. Exploring variations in both the depth and width of the model architecture or incorporating additional layers can significantly enhance feature capturing, thereby improving segmentation accuracy. Fine-tuning essential training parameters, such as learning rate and batch size, contributes to the model's convergence and overall performance. Additionally, the ensemble of multiple U-Net models can be employed to leverage diverse learning patterns and enhance segmentation robustness. Implementing post-processing techniques, such as morphological operations, can further refine the segmentation results.

VI. CONCLUSIONS

Our study illuminates the successful application of EfficientNet and U-Net models in the domains of brain tumor classification and segmentation. With accuracy rates of 99% and an impressive IoU score of 89%, these models demonstrate exceptional proficiency in precisely identifying and segmenting tumor regions within MRI images. This level of precision not only ensures meticulous tumor area identification but also holds promising implications for advancing brain tumor detection and monitoring.

Furthermore, the demonstrated resilience of both models in navigating intricate scenarios, including varying perspectives in MRI images, while maintaining heightened accuracy, underscores the robustness of deep learning in addressing the intricacies of brain tumor detection. The adeptness of these advanced techniques opens avenues for redefining medical imaging, offering the potential for automated detection systems through sophisticated image analysis and deep learning.

In conclusion, the effective implementation of EfficientNet and U-Net models, characterized by stellar accuracy, refined segmentation quality, and adaptability to diverse image types, underscores the transformative potential of deep learning in brain tumor classification and segmentation. These findings not only contribute to the current understanding of medical imaging but also pave the way for ongoing advancements, leveraging the sophisticated capabilities offered by deep learning methodologies.

VII. ACKNOWLEDGMENT

We very much appreciate the guidance and advice that Mr. Wahyono, S. Kom., Ph.D., throughout the Deep Learning course this semester. Thank you for all the knowledge that you have given to us.

We also are aware of the drawbacks that it isn't comparable to other research out there that uses complex neural networks and many more. However, throughout the final project completion, we are proud of what we can create and how it could be used and applied in real-world problems.

VIII. REFERENCES

- [1] Putri, R.C.A. (2022). Asuhan Keperawatan Pada NY. E Dengan Brain Metastase di Ruang Anggrek 2 RSUP dr. Sardjito. Poltekkes Kemenkes Yogyakarta.
- [2] Rahadi, F. (2023). Tantangan penanganan tumor otak di Indonesia. Republika Online.
- [3] Chatterjee, S. et al. (2022). Classification of brain tumours in MR images using deep spatiotemporal models. *Sci Rep* 12, 1505. doi: 10.1038/s41598-022-05572-6.
- [4] Miller, K.D. et al. (2021). Brain and other Central Nervous System Tumor Statistics. *CA: A Cancer Journal for Clinicians*, vol. 71, no. 5, pp. 381–406. doi:10.3322/caac.21693.
- [5] Nayak, D.R. et al. (2022). Brain Tumor Classification Using Dense Efficient-Net. *Axioms*, vol. 11, no. 34. doi:10.3390/axioms11010034.
- [6] Sajja, V.R. et al. (2021). Classification of Brain Tumors Using Fuzzy C-Means and VGG16. *Turkish Journal of Computer and Mathematics Education (TURCOMAT)*, vol. 12, no. 9, Apr. 2021, pp. 2103.
- [7] Das, S., Aranya, O. F. M. R. R., and Labiba, N. N. (2019). Brain Tumor Classification Using Convolutional Neural Network. 2019 1st International Conference on Advances in Science, Engineering and Robotics Technology (ICASERT), Dhaka, Bangladesh, pp. 1-5, doi: 10.1109/ICASERT.2019.8934603.
- [8] Kermi, A., Mahmoudi, I., and Khadir, M.T. (2019). Deep convolutional neural networks using U-Net for automatic brain tumor segmentation in multimodal MRI volumes. *Brainlesion: Glioma, Multiple Sclerosis, Stroke and Traumatic Brain Injuries*, pp. 37–48. doi:10.1007/978-3-030-11726-9_4.
- [9] Dong, H. et al. (2017). Automatic brain tumor detection and segmentation using U-Net based fully convolutional networks. *Communications in Computer and Information Science*, pp. 506–517. doi:10.1007/978-3-319-60964-5_44.
- [10] Nickparvar, M. (2021). Brain Tumor MRI Dataset. Kaggle. doi:10.34740/KAGGLE/DSV/2645886.
- [11] Tomar, N. (2022). Brain Tumor Segmentation. Kaggle.
- [12] Tan, M. and Le, Q.V. (2019). EfficientNet: Rethinking Model Scaling for Convolutional Neural Networks. *Proceedings of the 36th International Conference on Machine Learning*, 6105-6114.
- [13] Oloko-Oba, M., & Viriri, S. (2021). Ensemble of EfficientNets for the Diagnosis of Tuberculosis. *Computational intelligence and neuroscience*, 2021, 9790894. doi:10.1155/2021/9790894.
- [14] Alhichri, H. et al. (2021). Classification of Remote Sensing Images Using EfficientNet-B3 CNN Model with Attention. *IEEE Access*. PP. 1-1. doi:10.1109/ACCESS.2021.3051085.
- [15] Kashevnik, A. and Ali, A. (2022). 3D Vehicle Detection and Segmentation Based on EfficientNetB3 and CenterNet Residual Blocks. *Sensors*. 22. 7990. doi: 10.3390/s22207990.
- [16] Ronneberger, O., Fischer, P. and Brox, T. (2015). U-Net: Convolutional Networks for Biomedical Image Segmentation. *Lecture Notes in Computer Science*, pp. 234–241. doi:10.1007/978-3-319-24574-4_28.
- [17] Khouy, M. et al. (2023). Medical Image Segmentation Using Automatic Optimized U-Net Architecture Based on Genetic Algorithm. *J. Pers. Med.* 2023, 13, 1298. doi:10.3390/jpm13091298.